Electronic Supplementary Material (ESI) for Journal of Materials Chemistry C.

Supporting Information

Ultrasensitive Fe^{3+} Ion Detection Based on Carbon Quantum Dot-Functionalized Solution-Gated Graphene Transistors

Qin Fan,[a] Jinhua Li,*[a] Jianying Wang,[a] Zilu Yang,[a] Tao Shen,[a] Yizhong Guo,[b] Lihua Wang,[b] Muhammad Sultan Irshad,[a] Tao Mei [a] and Xianbao Wang *[a]

[a] *Hubei Collaborative Innovation Center for Advanced Organic Chemical Materials, Key Laboratory for the Green Preparation and Application of Functional Materials, Ministry of Education, Hubei Key Laboratory of Polymer Materials, School of Materials Science and Engineering, Hubei University, Wuhan 430062, P. R. China*
E-mail: jinhua_li@hubu.edu.cn (J.L.); wxb@hubu.edu.cn (X.W.)
[b] *Institute of Microstructure and Properties of Advanced Materials, Beijing University of Technology, Beijing 100124, P. R. China*

Materials and Reagents. The soda-lime glass substrate was purchased from the GULUO Company. Phosphate Buffered Saline was purchased from Sigma-Aldrich and stored at 4°C for future use. The single-layer graphene on copper foil was purchased from the VIGON Technology Company. Methanol, acetone, isopropanol, ethanol, benzaldehyde, sodium lignin sulfonate, p-phenylenediamine, aminobenzene boric acid, $FeCl_3$, $HgCl_2$, $CuCl_2$, $PbCl_2$, $CdCl_2$, AgCl, KCl, $CrCl_2$, $MnCl_2$, $CaCl_2$, $AlCl_3$, $BaCl_2$, $CoCl_2$, $NiCl_2$, $MgCl_2$, $FeCl_2$ and NaCl were purchased from Sinopharm. Polydimethylsiloxane (PDMS), mercaptoacetic acid (MAA), 1-(3-Dimethylaminopropyl)-3-ethylcarbodiimide hydrochloride (EDC), N-Hydroxy succinimide (NHS), polymethyl methacrylate (PMMA) were purchased from Aladdin. All the chemical reagents were of analytical grade and used without further purification. Ultrapure deionized (DI) water was used throughout the experiment.

Apparatus and Characterization. The morphologies and sizes of CQDs were characterized by transmission electron microscopy (TEM, FEI Themis 300 kV) under the accelerating voltage of 200 kV. For TEM analysis, the samples were prepared by the deposition of one drop of aqueous dispersion on a copper grid coated with thin film of carbon, and the solvent was removed by evaporation in air. The required photoluminescence (PL) and the luminescence decay profile were measured using a fluorescence spectrophotometer (PicoQuant Fluo Time 300). Fourier transform infrared spectrometry (FT-IR) was conducted on a Thermo Scientific NICOLET iS50 spectrometer using KBr pellets. Full range XPS survey spectra were tested on a Thermo Scientific Escalab 250xi XPS. Field emission scanning electron microscopy (FE-SEM) images were performed using a Zeiss Sigma 500, GRE at 10 kV. Besides, the graphene film was characterized by Raman spectroscopy (inVia Reflex) to examine the quality.

Preparation of CQDs. Sodium lignin sulfonate (10 mg) and p-phenylenediamine (20 mg) were dissolved in the solvent of 10 mL ethanol.[1] The obtained solution was transferred to a poly (tetrafluoroethylene) (Teflon)-lined autoclave (50 mL) and heated at 200ºC for 9 hours, and then allowed to cool to room temperature. The products were centrifuged at 12000 rpm for 10 minutes. The resulting suspensions containing CQDs

were filtered through 0.22 μm filter membranes and then subjected to dialysis (1,000 Da molecular weight cut off) about for 72 hours.

Device Fabrication. Fig. 2b shows the schematic diagram of the SGGT-based sensor. Patterned Au (~ 100 nm)/Cr (~ 10 nm) source, drain and gate electrodes were initially deposited on a glass or PET substrate via thermal evaporation with the aid of a shadow mask. The thin chromium layer serves as the adhesive layer to improve the adhesion of the Au layer on the substrate. Single-layer graphene was synthesized on copper foils by a CVD method.[2] The graphene film is mainly single-layer, which is confirmed by the Ramen spectrum which indicates the 2D peak with the height about two times of that of the G peak (Fig. S12).[3] A PMMA film (~ 500 nm) was spin coated on graphene and then annealed at about 100°C for 30 minutes. Afterwards, it was immersed in an aqueous solution of iron chloride to etch the Cu substrate and washed by distilled water. The graphene/PMMA film was then transferred onto the confined channel area between source and drain (0.2 × 6 mm). Moreover, the PMMA layer was dissolved and removed from graphene by acetone. The fabricated devices were transferred to a glove box filled with high purity of Ar intended for annealing at 200℃ for 1 hour. A PDMS wall was attached to the substrate to enable the test of the device in trace liquid (PBS solution).

Gate electrode Modification with CQDs. Au gate electrodes (0.3 cm × 0.3 cm) were firstly immersed in Piranha solution (H_2O_2/H_2SO_4, V/V = 3/1) and then polished to obtain mirror surface with 0.5 μm alumina power, followed by sonication in ethanol and water respectively. MAA (50 mM, 10 μL) was modified on the clean gate electrode in dark overnight to give carboxyl groups, a 10 μL of a mix-solution of EDC (0.2 mM, PBS solution, pH = 5.5) and NHS (0.5 mM, PBS solution, pH = 5.5) was introduced to the electrode surface to activate the carboxyl groups for 5 hours. The Au gate electrodes were washed with PBS buffer three times. CQDs water solution (1 mg/mL, 10 μL) was introduced to the electrode surface for 3 hours, and then clean it with PBS buffer for three times to remove unfixed CQDs and other residua on Au gate electrodes.

Device Test. All as-prepared electrodes were immersed in PBS (pH = 7.4) for 15 min to remove the residua before measurements. The SGGTs were tested at a fixed $V_D = 0.1$

V in a gate voltage range of 0 to 2 V at a sweeping rate of 0.02 V/s, and PBS was used as the electrolyte for all measurements. The device performance, including transfer curves (I_D vs V_G) and time-dependent channel currents (I_D vs time), was characterized by using two probe Keithley 2400 source meters controlled by a computer with a LabVIEW program. The detection limit of each device is defined by the channel current response at the condition of signal/noise > 3.

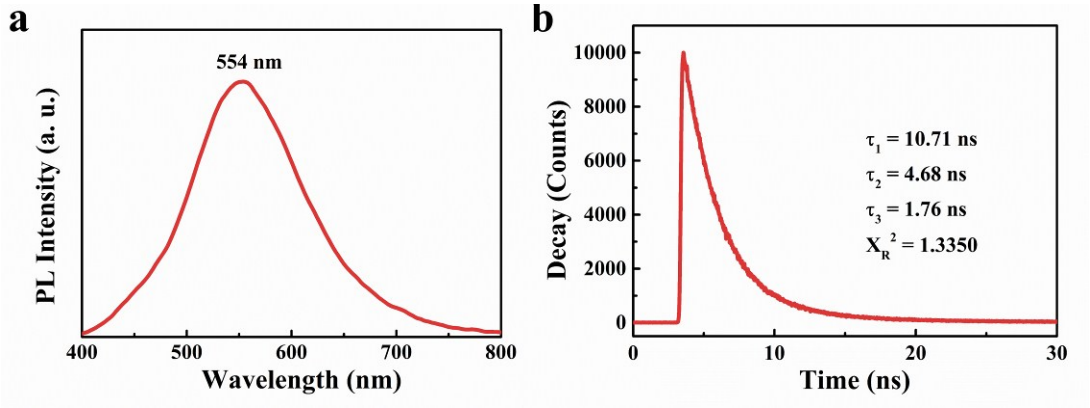

Fig. S1. (a) The PL spectrum of CQDs. (b) The luminescence decay profile of CQDs.

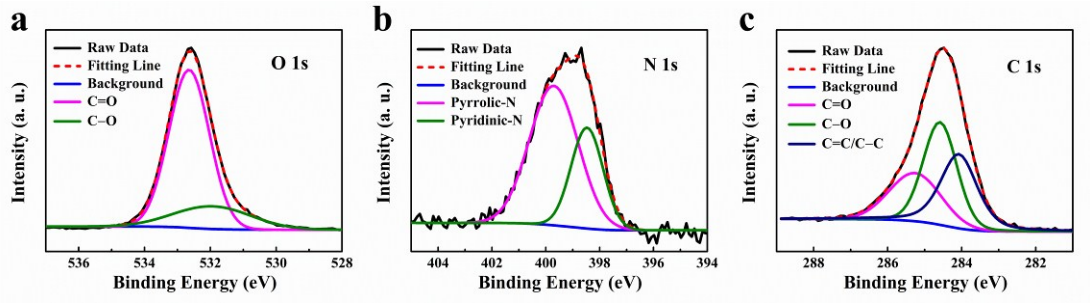

Fig. S2. (a) High-resolution O1s XPS spectrum of CQDs. (b) High-resolution N1s XPS spectrum of CQDs. (c) High-resolution C1s XPS spectrum of CQDs.

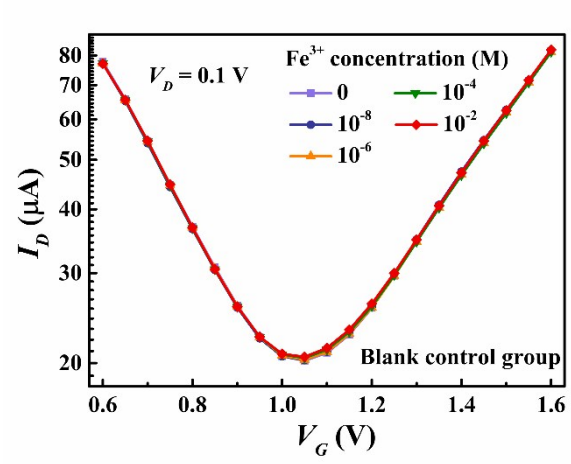

Fig. S3. The transfer curves of the control device after the addition of Fe^{3+} ions.

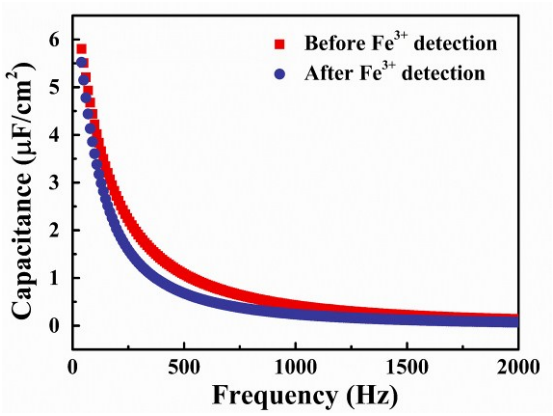

Fig. S4. The capacitance comparison of the Fe^{3+} ion sensor before and after Fe^{3+} ion detection.

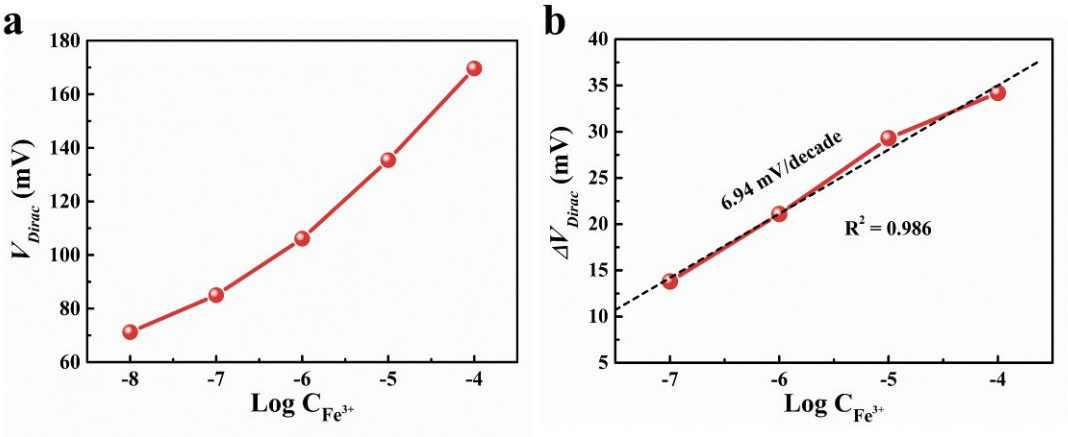

Fig. S5. (a) The Dirac voltage (V_{Dirac}) of the device versus the logarithmic value of Fe^{3+} ion concentration. (b) The Dirac voltage change (ΔV_{Dirac}) of the device versus the logarithmic value of Fe^{3+} ion concentration.

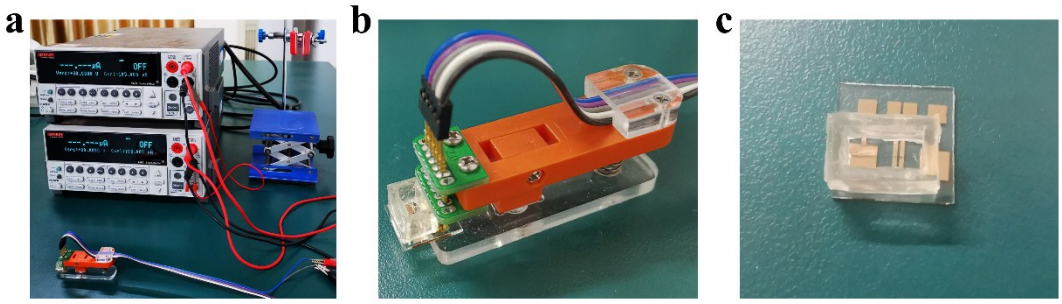

Fig. S6. Photographs of the SGGT device detection platform. (a) It consists of two connected Keithley 2400 source meters controlled by a computer and a SGGT device. (b) The SGGT device immersed in the PBS buffer and connected to the Keithley 2400 source meters. (c) The SGGT device with a PDMS well.

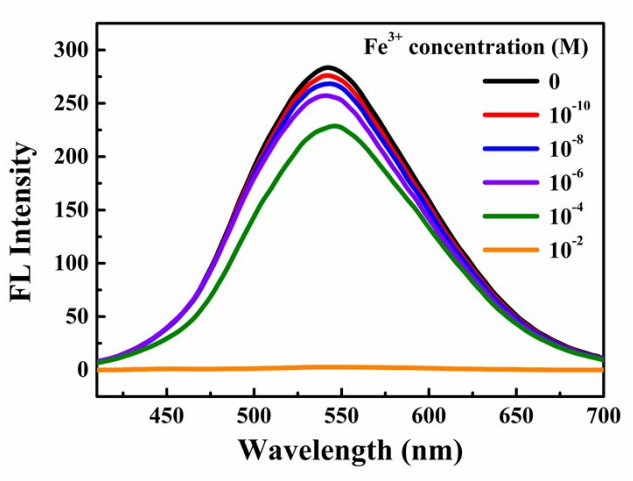

Fig. S7. FL emission spectra of the CQDs upon the addition of various concentrations of Fe^{3+} ions from 0 to 1.0×10^{-2} M.

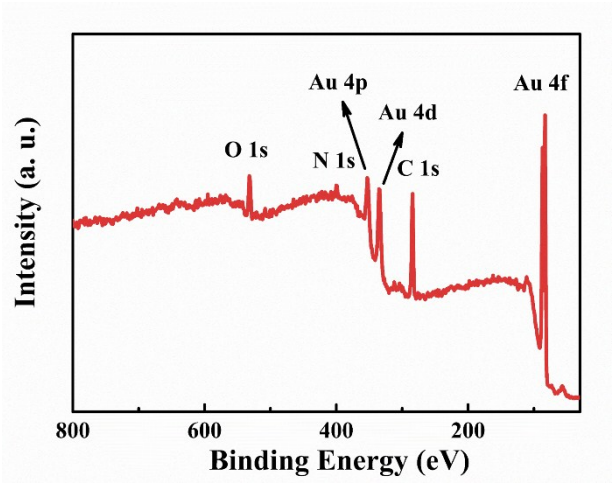

Fig. S8. Full range XPS survey spectrum of CQD-modified Au gate electrode.

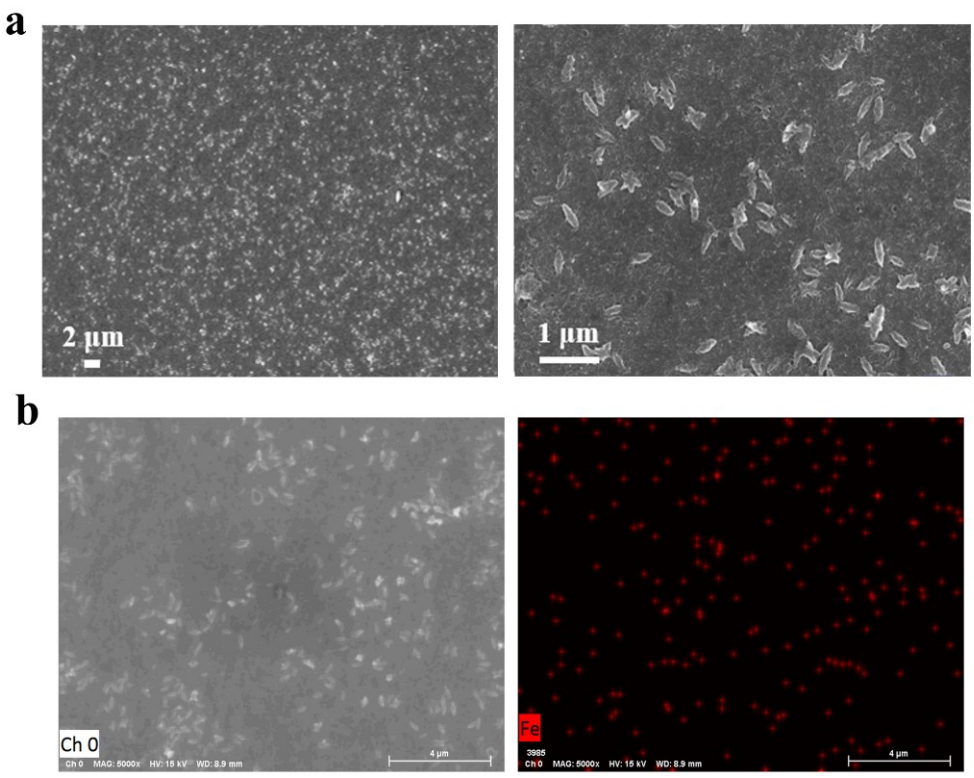

Fig. S9. (a) SEM image of the CQD-modified Au gate electrode after detecting Fe^{3+} ions. (b) Element mapping result of the CQD-modified Au gate electrode after detecting Fe^{3+} ions.

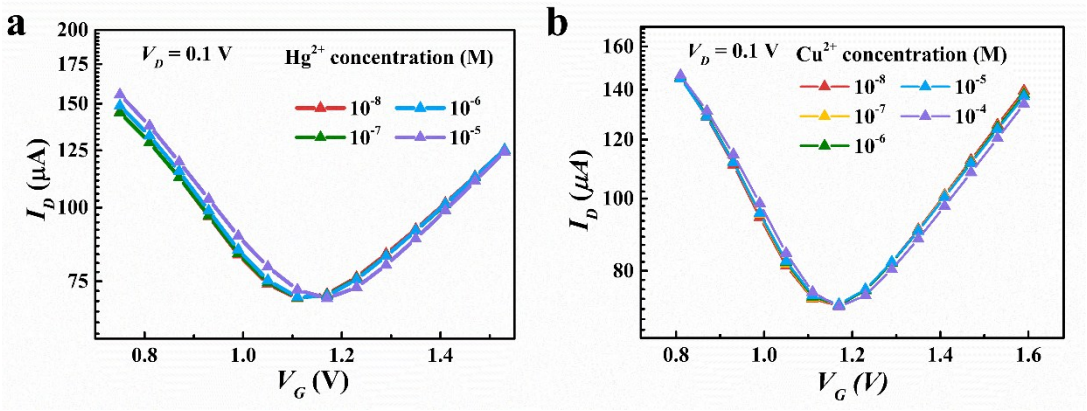

Fig. S10. (a) The transfer curves of the Fe^{3+} ion sensor after the addition of Hg^{2+} ions. d) The transfer curves of the Fe^{3+} ion sensor after the addition of Cu^{2+} ions.

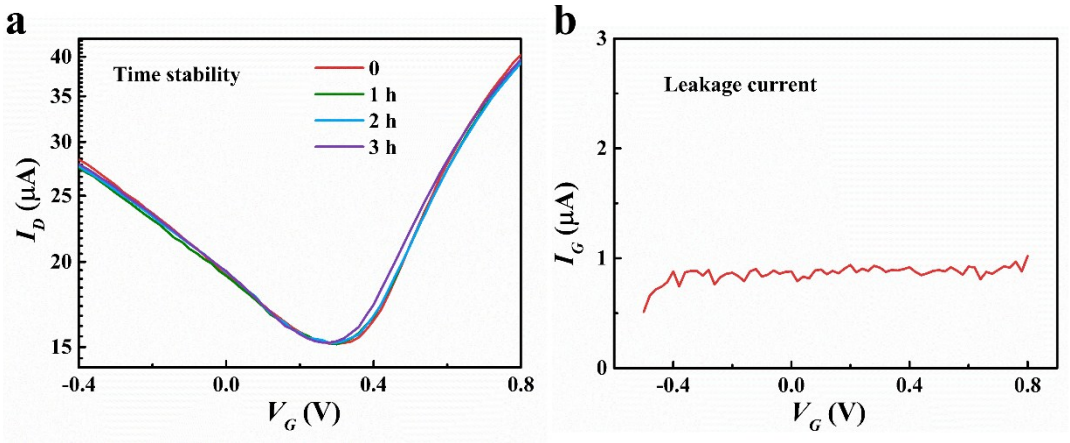

Fig. S11. (a) Time stability of the Fe^{3+} ion sensor. (b) Leakage current of the Fe^{3+} ion sensor.

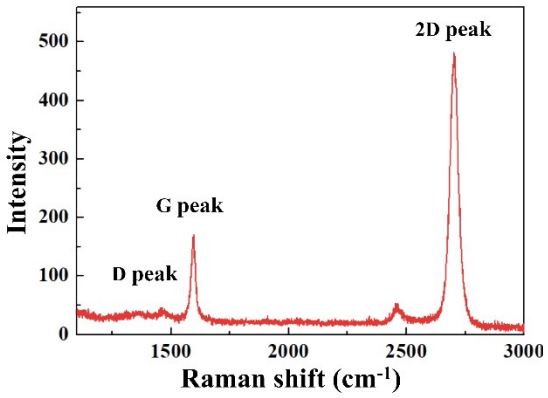

Fig. S12. Raman spectrum of a single-layer CVD graphene on Si substrate.

Table S1. Comparison on recently reported various methods for detection of Fe^{3+} ions.

Detection Method	Materials	LOD	Linear Range	Ref.
FET	γ-pyrone derivative	50 fM	50 fM – 5mM	4
Fluorescence	Oligofluoranthene	1.0 pM	62.5 pM – 3.1 mM	5
Fluorescence	SWNTs-deferoxamine	10 pM	–	6
Fluorescence	ATP	0.1 nM	1 − 10 nM	7
Fluorescence	Benzothiazole	0.61 nM	1 nM – 0.782 mM	8
Fluorescence	CDs	1.7 nM	5.0 nM – 0.1 mM	9
Fluorescence	N,P-CDs	1.8 nM	5 nM – 100 nM	10
Fluorescence	N-CDs	2.6 nM	0.1 – 25 μM	11
Colorimetry	Rhodamine B derivative	3.9 nM	0.5 – 50.0 μM	12
Fluorescence	Poly(9-fluorenecarboxylic acid)	7.4 nM	–	13
Fluorescence	DA-GQDs	7.6 nM	20 nM – 2 μM	14
Fluorescence	N,S-GQDs	8 nM	0.01 – 25.0 μM	15
Electrochemistry	TTA	8.3 nM	10 nM – 10 mM	16
Electrochemistry	Deferoxamine	10 nM	10 nM – 0.1 mM	17
Fluorescence	Copper nanoclusters	10 nM	10 nM – 10 μM	18
Fluorescence	BQR-6G	10 nM	0 – 14 μM	19
Fluorescence	Oligothiophene derivative	13.6 nM	0 – 5.0 μM	20
Fluorescence	N,S-CQDs	14 nM	1 – 500 μM	21
SGGT	CQDs-MAA	0.1 fM	1 pM – 1μM	This work

Abbreviations: FET, field-effect transistor; SWNTs, single-walled nanotubes; ATP, adenosine-5′-triphosphate; CDs, carbon dots; DA, dopamine; GQDs, graphene quantum dots; TTA, tris(3-(thiophenol)propyl)amine; BQR, benzothiazole quinoline rhodamine; SGGT, solution-gated graphene transistor; CQDs, carbon quantum dots.

Notes and references

1 X. Zhu, J. Wang, Y. Zhu, H. Jiang, D. Tan, Z. Xu, T. Mei, J. Li, L. Xue, X. Wang, *Microchim. Acta* 2018, **185**, 510.

2 a) Z. Sun, Z. Yan, J. Yao, E. Beitler, Y. Zhu, J. M. Tour, *Nature* 2010, **468**, 549; b) R. X. He, P. Lin, Z. K. Liu, H. W. Zhu, X. Z. Zhao, H. L. Chan, F. Yan, *Nano Lett.* 2012, **12**, 1404; c) F. Yan, M. Zhang, J. H. Li, *Adv. Healthcare Mater.* 2014, **3**, 313.

3 M. J. Allen, V. C. Tung, R. B. Kaner, *Chem. Rev.* 2010, **110**, 132.

4 T. D. Nguyen, A. Labed, R. El Zein, S. Lavandier, F. Bedu, I. Ozerov, H. Dallaporta, J. M. Raimundo, A. M. Charrier, *Biosens. Bioelectron.* 2014, **54**, 571.

5 X. G. Li, Y. Z. Liao, M. R. Huang, V. Strong, R. B. Kaner, *Chem. Sci.* 2013, **4**, 1970.

6 W. Cheung, M. Patel, Y. Ma, C. Yuan, Q. Xie, J. Lockard, G. Yuan, H. He, *Chem. Sci.* 2016, **7**, 5192.

7 Y. Yang, X. Y. Wang, Q. L. Cui, Q. Cao, L. D. Li, *ACS Appl. Mater. Interfaces* 2016, **8**, 7440.
8 H. Zhang, G. Zhang, J. K. Xu, Y. P. Wen, B. Y. Lu, J. Zhang, W. C. Ding, *Sens. Actuators, B* 2016, **230**, 123.
9 X. M. Yang, Y. Zhuo, S. S. Zhu, Y. W. Luo, Y. J. Feng, Y. Dou, *Biosens. Bioelectron.* 2014, **60**, 292.
10 B. F. Shi, Y. B. Su, L. L. Zhang, M. J. Huang, R. J. Liu, S. L. Zhao, *ACS Appl. Mater. Interfaces* 2016, **8**, 10717.
11 C. P. Han, R. Wang, K. Y. Wang, H. T. Xu, M. R. Sui, J. J. Li, K. Xu, *Biosens. Bioelectron.* 2016, **83**, 229.
12 L. F. Zhang, J. L. Zhao, X. Zeng, L. Mu, X. K. Jiang, M. Deng, J. X. Zhang, G. Wei, *Sens. Actuators, B* 2011, **160**, 662.
13 Y. Gao, H. M. Liu, Q. L. Liu, W. Wang, *Tetrahedron Lett.* 2016, **57**, 1852.
14 A. D. Chowdhury, R. A. Doong, *ACS Appl. Mater. Interfaces* 2016, **8**, 21002.
15 C. Shen, S. Y. Ge, Y. Y. Pang, F. N. Xi, J. Y. Liu, X. P. Dong, P. Chen, *J. Mater. Chem. B* 2017, **5**, 6593.
16 H. A. Zamani, M. R. Ganjali, F. Faridbod, M. Salavati-Niasari, *Mater. Sci. Eng., C* 2012, **32**, 564.
17 L. R. Kindra, C. J. Eggers, A. T. Liu, K. Mendoza, J. Mendoza, A. R. K. Myers, R. M. Penner, *Anal. Chem.* 2015, **87**, 11492.
18 H. Y. Cao, Z. H. Chen, H. Z. Zheng, Y. M. Huang, *Biosens. Bioelectron.* 2014, **62**, 189.
19 S. Das, K. Aich, S. Goswami, C. K. Quah, H. K. Fun, *New J. Chem.* 2016, **40**, 6414.
20 L. X. Lan, Q. F. Niu, Z. R. Guo, H. X. Liu, T. D. Li, *Sens. Actuators, B* 2017, **244**, 500.
21 H. F. Wu, J. H. Jiang, X. T. Gu, C. L. Tong, *Microchim. Acta* 2017, **184**, 2291.